Optical parametric sources from the SWIR to the LWIR for standoff gas sensing

Jean-Michel Melkonian, Jonas Hamperl, Quentin Berthomé, Jean-Baptiste Dherbecourt, Rosa Santagata, Myriam Raybaut, Antoine Godard

Optical parametric sources from the SWIR to the LWIR for standoff gas sensing

Jean-Michel Melkonian*, Jonas Hamperl, Quentin Berthomé, Jean-Baptiste Dherbecourt, Rosa Santagata, Myriam Raybaut, and Antoine Godard
DPHY, ONERA, Université Paris Saclay, F-91123 Palaiseau, France

ABSTRACT

We present our activities on the development of narrow linewidth tunable optical parametric sources and their integration in lidar systems. In particular, we present different implementations of the nested cavity optical parametric oscillator (NesCOPO) that enables tunable single-frequency emission from the SWIR to the LWIR, when pumped by a fixed or a tunable wavelength laser beam. We show how to amplify the output energy and while preserving the spectral linewidth to perform standoff detection of greenhouse gases and toxic chemicals with direct detection lidars.

Keywords: lidar, absorption spectroscopy, infrared, greenhouse gases

1. INTRODUCTION

Standoff detection of chemical species –particularly in the gaseous phase– is of interest for atmospheric research and Earth observation (monitoring of greenhouse gases), industrial process monitoring, defense and security (detection of chemical warfare agents or chemicals considered as such), and safety (leaks of hazardous gases). To this end, infrared absorption spectroscopy is probably the most powerful tool to identify chemical species since most polyatomic molecules display characteristic absorption features linked to their vibrational and rotational modes and thus to their chemical structure. Quantification is also possible provided that the absorption cross-sections have been measured beforehand.

For long range detection (from 100 m to several tens of kilometers), the choice of wavelengths is bounded by atmospheric transmission windows, roughly located between 2 and 2.5 µm (short wave infrared, SWIR), 3–4 and 4.5–5 µm (midwave infrared, MWIR) and between 8 µm and 13 µm (longwave infrared, LWIR).

Passive methods, relying on spectral analysis of absorbed solar or thermal light, by selection with optical filters, angular dispersion with grating or prisms, or interferometers, are now well established, having given rise to many commercial products and several spaceborne instruments. On the other hand, active methods, such as absorption lidars [1], provide a measurement independent from the optical background, while the spectral selectivity can be enhanced by using wavelength-tunable, narrow-linewidth lasers.

In spite of the increasing variety of devices emitting infrared light (solid state lasers, rare earth doped or supercontinuum fiber lasers, semiconductor quantum cascade lasers, optical parametric devices), it is still a challenge to emit a narrow linewidth radiation with a large wavelength tunability, especially when high peak powers are involved.

In this paper, we will review our recent work on narrow linewidth tunable optical parametric sources and their integration in lidar systems, for diverse applications such as methane leak detection for industrial safety, ground-based and airborne carbone dioxide and isotopic water monitoring, and detection of chemical warfare agents.

1.1. Principle of differential absorption lidars

In this work, we focus on differential absorption lidars (DIAL) that use attenuation and time-of-flight measurement of light pulses backscattered after propagation in the atmosphere (Figure 1). Return light flux is directly detected by a photodiode, in contrast with coherent lidars that use heterodyne schemes (usually to retrieve wind speed from the Doppler shift). In its simplest form, a DIAL emits two laser pulses consecutively at two different wavelengths. One

*jean-michel.melkonian@onera.fr

wavelength is in coincidence with an absorption band for the targeted species called λ_{ON}, and a second wavelength is on a minimum of absorption called λ_{OFF}. The laser pulses, after passing through the target gas cloud, are backscattered by the aerosols (dust or water droplets), collected by a telescope and focused on a photodetector. The gas concentration $C(z)$ at distance z is then retrieved from the ratio of the ON and OFF backscattered signals at time t such that $z = c\,t/2$, where c is the speed of light. Spatial resolution along the line of sight is usually limited by the detector bandwidth Δf, so that $\Delta z \cong c/2\Delta f$. If light is backscattered from a solid target, spatial resolution is lost and the ratio of the ON and OFF signals is equal to the integrated optical depth along the line of sight (IPDA configuration for Integrated Path Differential Absorption LIDAR). For the same distance, the IPDA signal is typically 10^4 higher than the DIAL signal. Obviously, additional ON wavelengths are required for identification of more than one molecule, or if atmospheric species present infrared spectra overlapping with the one from the target. Additional OFF wavelengths can also be useful for better subtraction of the baseline on large spectral ranges, using a polynomial fit. Note that wavelength tunability does not need to be continuous, because for most applications the measurement of the shape of the absorption line is not necessary to retrieve the concentration (unless pressure and temperature are unknown and suspected to vary greatly).

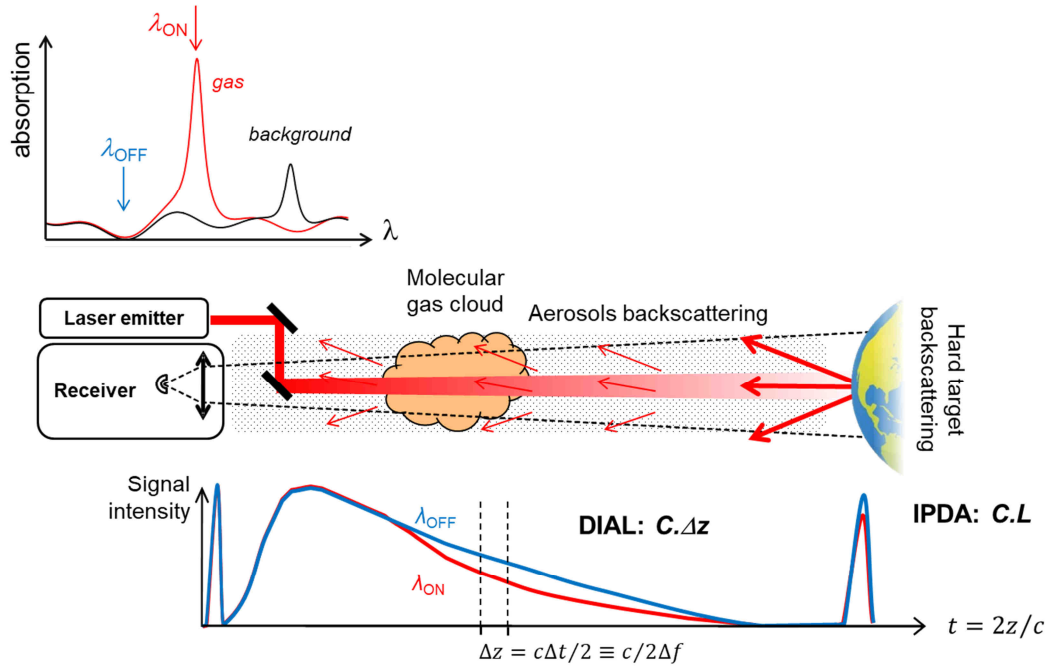

Figure 1. Simplified principle of molecular detection with a differential LIDAR.

1.2. Challenges for absorption lidar emitters

As for any lidar, a DIAL emitter should deliver a high peak power laser beam with a good pointing stability and a low divergence. In addition, the light spectrum should match the absorption spectrum of the target molecules, i.e. it should be very narrow and centered at a very precise wavelength, and at least tunable over two wavelengths for the ON/OFF differential scheme to work. This last requirement can take very different forms depending on how many different species are addressed, the complexity of their chemical composition, air pressure that has a strong impact on the absorption linewidth, and the abundance of the target species relatively to the one of other species with similar spectral features. We have listed nonetheless a few typical requirements in Table 1, to appreciate how difficult it may be to meet them all at once.

Two extreme examples can be found in remote sensing of CO_2 from space, and chemical warfare agents (CWAs) detection. For the former, a pulse energy above 50 mJ is required to get enough signal from Earth reflection after at a 10 km altitude, while the wavelength stability must be better than 1 MHz to get the required precision, taking into account the effect of pressure with the altitude [2]. For the latter, an ON/OFF tunability of 50 cm^{-1} and a global tunability of ~500 cm^{-1} are required because CWAs display broad spectral absorption bands, and what is the more, in the LWIR.

To be able to address these different challenges, we have developed generic optical architectures based on down-conversion of light in nonlinear crystals under laser pumping, as described in the next section.

Table 1. Typical challenges for DIAL emitters.

Parameter	**Typical value**	**Most challenging requirement**
Pulse energy *(peak power for 20 ns pulses)*	1 mJ *(50 kW)*	50 mJ *(2,5 MW)*
Pulse duration *(equivalent range resolution)*	< 100 ns *(15 m)*	< 20 ns *(3 m)*
M^2	< 2	< 2
Number of laser lines	> 2	> 8
Wavelength linewidth	< 1 GHz	< 100 MHz
Wavelength stability	< 20 MHz	< 1 MHz
ON/OFF wavelength tunability	0.7 cm^{-1} (20 GHz)	50 cm^{-1}
ON/OFF switching speed	> 100 Hz	500 Hz
Wavelength tunability for multi-species detection	Several cm^{-1} (not continuous)	500 cm^{-1} (not continuous)

2. ENABLING TECHNOLOGIES

2.1. Quasi-phase-matched crystals

To generate radiation in the mid-infrared, we use frequency down-conversion of the pump in non centro-symmetric crystals, using second-order $\chi^{(2)}$ nonlinearity, so that $\omega_p \rightarrow \omega_s + \omega_i$, where ω is the optical frequency and the indices *p*, *s*, *i* stand for the pump, signal and idler respectively. Efficient conversion occurs when the signal and idler waves propagate in phase with the nonlinear polarization created by the pump, which is naturally prevented by chromatic dispersion. Birefringent phase-matching, which uses the dependence of the index of refraction to compensate for chromatic dispersion, is a method that can be implemented in all anisotropic crystals. We use it for large aperture crystals in nonlinear amplifiers, such as $KTiOPO_4$, $ZnGeP_2$, and CdSe. However, this method does not give access to the highest coefficient d_{33} of the nonlinear tensor which is associated to identical polarizations, and the efficiency is further reduced by spatial walk-off between the waves, which is another consequence of birefringence. Besides, birefringence phase matching is not possible is cubic crystals such as ZnSe or GaAs, despite their high $\chi^{(2)}$ non-linearity.

In all our nonlinear oscillators we now use quasi-phase-matched (QPM) crystals, in which the nonlinear coefficient is periodically reversed to cancel the phase-mismatch whenever it reaches π. This allows using waves with identical polarizations (a.k.a. Type 0 phase matching) and a single propagation direction. This writes:

$$k_p - k_s - k_i - \frac{2\pi}{\Lambda} = 0, \tag{1}$$

where *k* is a wavevector and Λ is the QPM grating period. QPM has been a decisive technology to be able to use small beam sizes and hence low laser energies. QPM offers unique phase matching engineering possibilities, such as multiple periods and fan-out gratings for changing the wavelength by translating the crystal, or aperiodic grating to widen the

acceptance bandwidth (Figure 2). We will give practical implementations of these three kinds of gratings in the next sections. In addition, wavelength tuning can be achieved by temperature control of the crystal. Periodic reversal can be provoked in ferroelectric crystals such as MgO:$LiNbO_3$ or Rb:$KTiOPO_4$ by domain propagation under a strong electric field (resulting in MgO:PPLN and PPRKTP respectively), or in cubic crystals such as GaAs by patterning using lithography and etching and then epitaxy regrowth (resulting in OP-GaAs). The materials have not been listed in an exhaustive way.

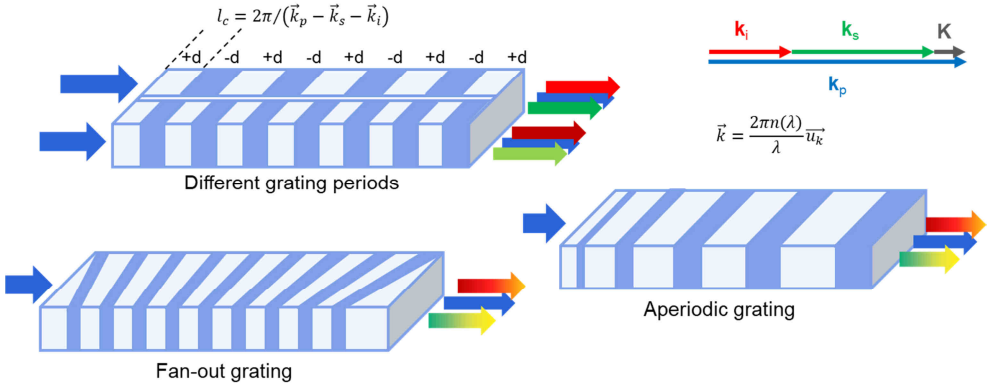

Figure 2. Three types of quasi-phase matching designs actually used in lidar emitters.

QPM can also be implemented for waves of different polarizations. In the case of crossed signal and idler polarizations (a.k.a. Type II phase matching), the acceptance bandwidth gets much narrower than for identical polarizations, which can be of great use to generate narrow linewidth radiation near the degeneracy $\omega_s = \omega_i = \omega_p/2$. Since spatial walk-off remains zero, a longer crystal can be used to compensate for the lower nonlinear efficiency. In Figure 3, we compare the acceptance bandwidths of PPLN pumped at 1.064 µm for an idler wavelength near 2.3 µm for type 0 and type II phase matching: the contrast is striking. This is why we often chose type II for our emitters operating close to degeneracy (at least when the idler is below 3 µm). Another solution is to put a volume Bragg grating (VBG) inside the NesCOPO cavity: this element clearly hinders the wide tunability of the NesCOPO, but the spectral filtering is so efficient that the crystal can be used in Type 0 QPM (Figure 3).

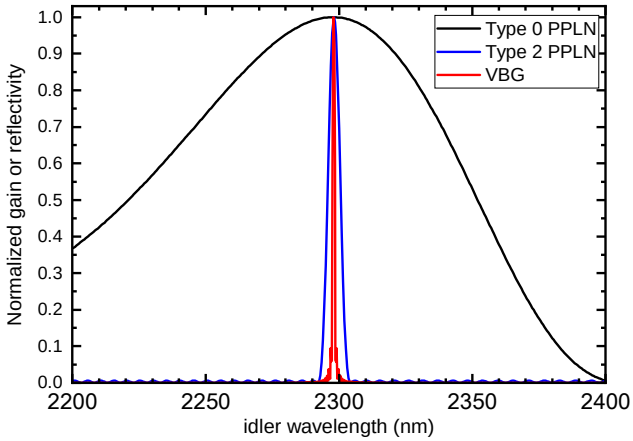

Figure 3. Calculated spectral gain of PPLN for type 0 and type 2 phase matching (single-pass low signal parametric gain), and normalized reflectivity of a VBG for comparison (2.5 mm thick, 400 ppm index modulation, reflectivity is 79%).

Another interesting case is backward QPM, in which one of the generated waves propagates in the direction opposite to the pump (one $\vec{k}$ is replaced by $\overrightarrow{-k}$ in Eq. (1)). Although proposed very early, this has only been experimentally demonstrated recently thanks to PPRKTP, because the small required QPM period of about 500 nm would make the

domains merge in PPLN [3]. A backward OPO oscillates without mirrors, it has no longitudinal mode just like a DFB laser, and the spectrum of the backward wave is transform-Fourier limited. However, wavelength tuning of the backward wave needs a tunable pump wavelength, because it is quite insensitive to temperature.

A peculiarity of QPM is that if the crystal is not cut right after a domain border, the three waves will not be in phase anymore, so a special trick is necessary if one wants to cascade several QPM crystals, as will be discussed below.

2.2. The nested-cavity optical parametric oscillator

Pulsed OPOs are not notoriously known for generating narrow-linewidth, diffraction-limited beams. This is because of the absence of spectral and spatial selection in the cavity, and the use of short cavities (to build up the field during the transient travelling of the pump) and large beam sizes to carry more energy. We have solved this problem by designing a low-threshold oscillator with embedded spectral filtering [4], and amplification of its output in large aperture crystals (see next section).

The nested-cavity optical parametric oscillator (NesCOPO) is based on a dual-cavity doubly resonant scheme where the signal and idler waves oscillate in separated cavities, as depicted in Figure 4. Pairs of mirrors M2-M3 and M1-M3 are related to the signal and idler cavities, respectively. A double-pass pump beam is made possible owing to the gold-coated mirror M3. Such a configuration is suitable to achieve a low oscillation threshold and to prevent back conversion toward the pump after reflection onto M3, providing that the relative phase between the three interacting fields is maintained at its optimal value in the backward direction. This condition can be fulfilled by cutting the crystal after a domain end, or, in a more practical way, by adjusting the transverse position of a wedged PPLN crystal. In this case, the OPO gain bandwidth is halved while the threshold is divided by four compared to the single-pass scheme.

Adequate differentiation and separate adjustment of both signal and idler cavities enables single-longitudinal-mode emission because only one single exact coincidence of signal and idler modes is obtained within the parametric gain bandwidth (see Figure 4, right). This is analogous to the mechanical Vernier effect.

In marked contrast with injection-seeded OPOs, whose tunability is restricted to the one of the seeding laser, usually a DFB diode, the NesCOPO tunability is only limited by the phase-matching properties of the crystal, which is much larger. When a quasi-phase-matched crystal (QPM) is used, the wavelength boundaries are only limited by the transmission curves of the mirrors, because QPM allows defining several phase-matching setpoints in a single crystal (see Sec. 2.1).

Mode-hop frequency tuning of the radiation can be obtained by adjusting only one parameter (signal or idler cavity length, crystal temperature, change of QPM period by transverse translation of the crystal, or pump frequency) whereas fine continuous tuning is obtained by adjusting simultaneously two parameters so as to maintain the doubly resonant oscillation on the same mode coincidence. The choice in the adjustment parameter actually defines the span and speed of wavelength tuning:

- Change of QPM period by crystal translation (~ 1 sec): to change the target spectral range by a few cm^{-1} or up to several hundreds of cm^{-1}, e.g. to switch the emitter between species (i.e. $CO_2 \rightarrow H_2O$);
- Change of crystal temperature by thermoelectric heating/cooling (~ 1 min): to set the QPM wavelengths to their targets, as in a calibration process, and/or to extend the spectral ranges offered by the different QPM periods;
- Signal or idler cavity length by piezoelectric actuation (~ 1 ms): to switch between close wavelengths (fitting within the acceptance bandwidth of the oscillator crystal, which is typically 1 cm^{-1}), e.g. to perform a differential ON/OFF measurement;
- Pump frequency tuning (time depends on laser technology): any of the aforementioned uses;
- Signal and idler cavity length: to scan several wavelengths across an absorption linewidth.

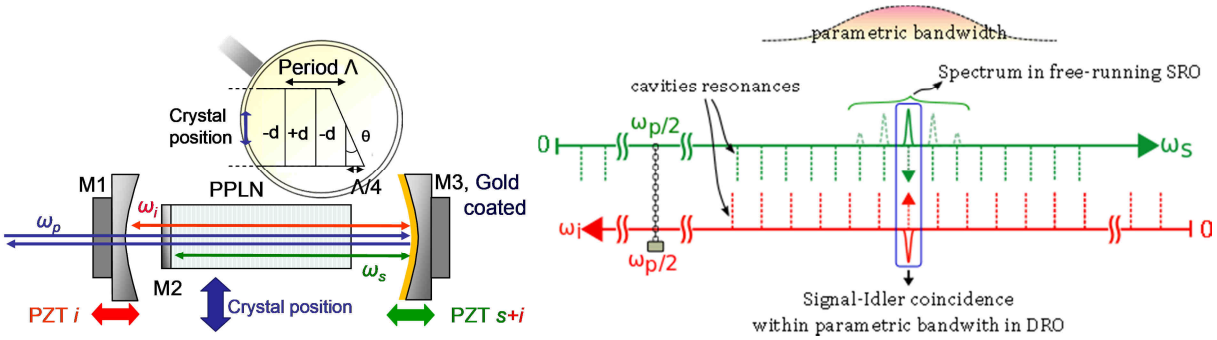

Figure 4. Principle of the nested cavity optical parametric oscillator (NesCOPO).

The huge wavelength versatility of the NesCOPO has a downside though: the wavelength must be measured very precisely. On the other hand, as it operates on a single longitudinal mode within a spectral window that is know from the crystal QPM period and temperature, a full spectrum analyzer is not necessary. A combination of Fizeau interferometers [5] or Fabry-Perot interferometers [6], an integrated Fourier Transform Spectrometer [7], or mode beating with a frequency comb [8] are all suitable methods.

Note that if the gain bandwidth is especially large, the Vernier effect will fail to select only one coincidence: thus is why we have to resort to Type II phase matching when the signal and idler wavelength are close to the degeneracy point (2.128 µm for 1.064 µm pumping). We also investigated the use of a VBG as the output coupler M3 for the idler wave, to reduce the spectral acceptance of the cavity and be able to use a Type 0 PPLN crystal. The NesCOPO operated on a single longitudinal mode and could be tuned over 15 nm thanks to a transverse chirp of the Bragg period [9].

2.3. Optical parametric amplifiers

The general architecture of our emitters is the one of a Master–Oscillator–Power–Amplifier (MOPA). The spectral and spatial characteristics of the beam are defined by the master oscillator (the NesCOPO described in Sec. 2.2), and are preserved through amplification, provided that pump lasers have adequate spatial and spectral features, and that full saturation is not reached. The superiority of this approach was experimentally demonstrated by others 14 years ago [10]. In our SWIR/MWIR emitters, we start from a commercial diode-pumped, injection-seeded Nd:YAG laser to pump a NesCOPO, usually based on PPLN, with less than 1 mJ of energy at 1.064 µm (Figure 5a). The rest of the laser energy is used to pump several crystals (usually PPKTP), separated by a signal/idler dichroic mirror to mitigate backconversion effects occurring when the three waves are not in phase at the input of a crystal, or when the pump becomes depleted near the center of the beam. After that, LWIR radiation can be generated by difference frequency in a crystal such as $ZnGeP_2$, as we have shown previously and will not be detailed here [11]. The MOPA concept can be transposed further into the infrared by choosing adequate optics and crystals (Figure 5b). However, the scarcity of high-energy single-frequency 2 µm lasers make the LWIR energy more difficult to scale up. Experimental implementations of these architectures are given in the next section.

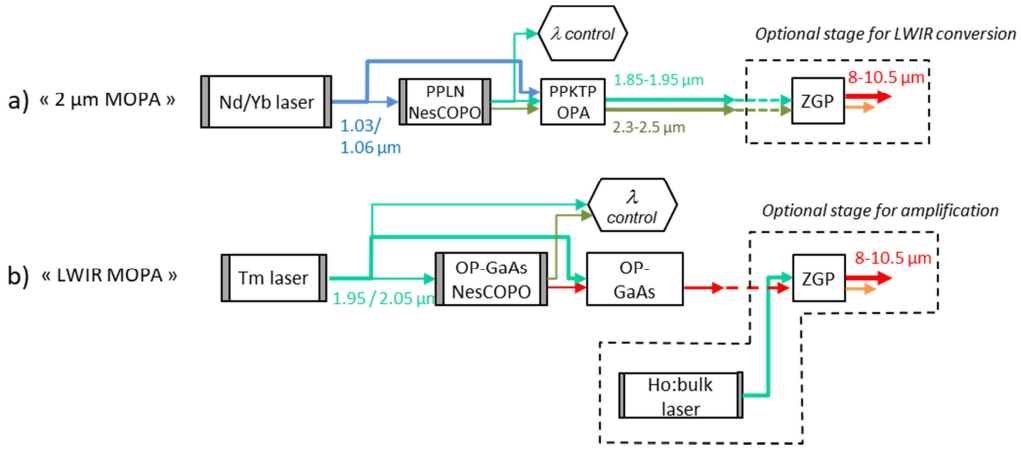

Figure 5. Two MOPA architectures for SWIR (or MWIR) and LWIR generation.

3. EXAMPLES OF LIDAR EMITTERS

3.1. 2 µm emitter for ground-based water vapor isotope ratio measurements

So far, no DIAL instrument has been able to quantify the relative abundance of the water isotopologue $HD^{16}O$, which would require collocated measurements of both the main isotopologues $H_2{}^{16}O$ and $HD^{16}O$. Such a measurement would lead to improved understanding of processes governing the global hydrological cycle, with the prospects of improving the accuracy in the predictions made by atmospheric general circulation models [12, 13]. To this aim, we realized a parametric source operating at 1.98 µm and performed a first demonstration of probing $H_2{}^{16}O$ and $HD^{16}O$.

The emitter architecture is of the "2 µm MOPA" type described in Figure 5a. It is an improved, more ruggedized, version of our previous MOPA setups [11, 14, 15]. A picture of the setup is shown in Figure 6. The parametric source is based on a NesCOPO combined with OPA stages, pumped by a commercial injection-seeded Nd:YAG laser (Innolas), delivering 12 ns-pulses at a repetition rate of 150 Hz. The NesCOPO uses a MgO:PPLN crystal in type II phase-matching (crossed idler and signal polarization), and emits single-frequency radiation, tunable in a 1 nm-window around 1982.5 nm (signal) suitable for addressing $H_2{}^{16}O$ and $HD^{16}O$ (the idler wavelength lies around 2298 nm but is not used for the measurement). The OPA uses several rubidium doped, periodically poled, KTP nonlinear crystals (PPRKTP). These crystals combine a high damage threshold (> 4 J/cm² with coating), a high nonlinearity (d_{eff} > 9 pm/V), and the possibility to be poled through thick aperture (up to 5x5 mm²) [16]. With a pump energy of 70 mJ, and idler rejection between the last two crystals (total interaction length of 30 mm), it was possible to obtain a signal energy in the range of 6–9 mJ at 1982 nm.

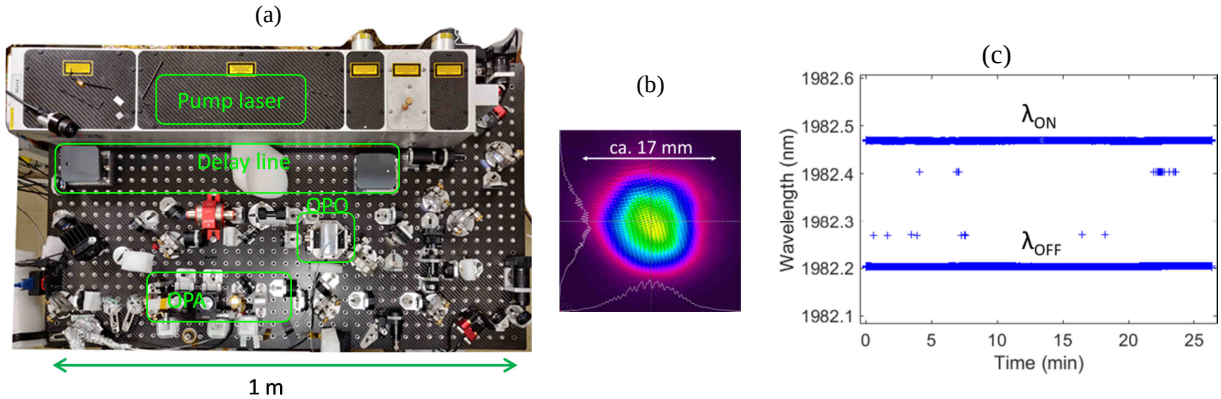

Figure 6. Experimental bench of the parametric laser source. (b) Transverse beam profile at the laser bench output. (c) λ_{ON} / λ_{OFF} recorded wavelength switching for $HD^{16}O$ measurement

The NesCOPO emitted wavelength is pulse-to-pulse modulated and recorded with a High Finesse WS6 IR wavemeter (Figure 6c). For each targeted species ($H_2{}^{16}O$ and $HD^{16}O$), such pulse-to-pulse wavelength modulation is necessary to emit the two wavelengths (namely λ_{ON} and λ_{OFF}) in and out of coincidence with the absorption line. This is performed by adjusting the NesCOPO cavity length using piezoelectric transducers. A transverse profile of the output beam after passing through a beam expander is shown in Figure 6b. It is Gaussian with a measured M^2<1.5 and a divergence full-angle of 300 µrad. The emitter is mounted on a carbon fiber bench (CarbonVision) to minimize temperature induced deformation. Even so, the pump beam is continuously monitored by two cameras to monitor beam pointing drift during the day as the lidar is tested in an unregulated temperature environment.

The lidar receiver consists of a 10-inch, custom-made Newtonian telescope which focuses the backscattered radiation onto a 900 µm-multimode fiber, whose output is imaged onto a commercial InGaAs amplified PIN photodiode of 300 µm diameter. The signal is pre-amplified and digitized with a high-speed 12 bit oscilloscope card, for a total NEP of 1.3 pW/√Hz and a bandwidth of 3.5 MHz (50 m longitudinal resolution). The telescope full-field-of view angle is 1.2 mrad.

DIAL tests along a horizontal path were conducted on 16 April 2021 in Palaiseau, France. The upper panels of Figure 7 show the recorded ON/OFF lidar signals expressed as signal-to-detection-noise ratio (SNR), with a dominant noise contribution from the transimpedance amplifier. The lower panels of Fig. 77 show the retrieved volume mixing ratios (VMR). The signals were averaged over 30 minutes successively for each species. For $H_2{}^{16}O$, a reference was provided by an in-situ Picarro G2401 analyzer, located in the vicinity of the lidar instrument.

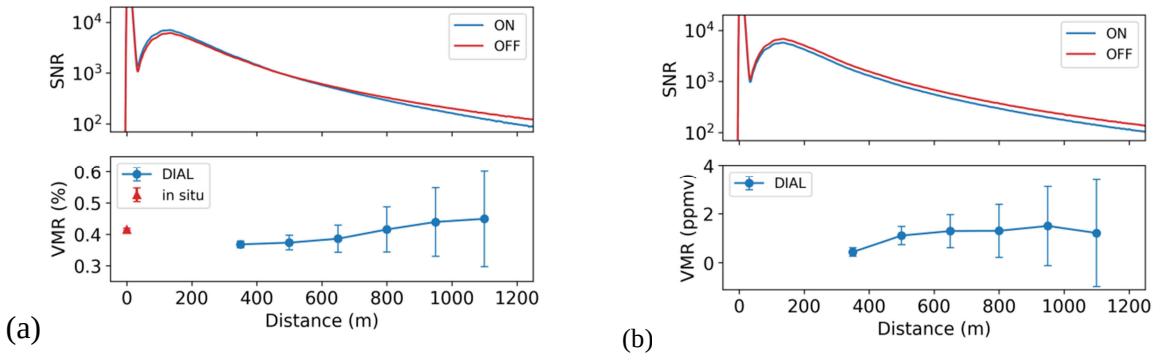

Figure 7. Raw (no energy normalization) averaged DIAL signals over 30 min and retrieved VMR for $H_2{}^{16}O$ (a) and $HD^{16}O$ (b).

We recently integrated the DIAL emitter in a mobile truck combined with a zenith-looking telescope in order to measure vertical profiles of $H_2{}^{16}O$ and $HD^{16}O$ in the lower troposphere. We will compare the DIAL measurements with those obtained by a Raman lidar and in-situ sensors in order to quantify instrument errors and biases and compare them with theoretical simulations [13]. Future work will also consist in increasing the extracted power of the transceiver for higher sensitivity.

3.2. 2 µm emitter for airborne measurements

Although the possibility to measure greenhouse gases from air and space with lidars is expected to come with significant benefits such as measurement independency from solar illumination, the technical and scientific challenges for this kind of mission are highly demanding. In this section, we give an overview of our ongoing efforts to increase the technical readiness level of a lidar that is intended for multi-species detection in airborne operation. These technical developments are being carried initially for an ESA TRP project (GENUIN) and now running in the frame of the EU H2020 LEMON project [17] in collaboration with climate research laboratories. The lidar is designed for vertical DIAL measurement of water vapor and its isotope HDO, as well as carbon dioxide.

The infrared emitter is based on the combination of two NesCOPOs with a single optical parametric amplifier line as illustrated in Figure 8. The pump laser is an injection-seeded, diode-pumped actively Q-switched Nd:YAG laser based on a stable resonator and a Nd:YAG amplifier, yielding 15 ns long pulses and operating at a 150 Hz average repetition rate. The NesCOPOs are pumped by a beam extracted directly from the oscillator to ensure a high beam quality in the

focused far field. In the first NesCOPO, the QPM condition is tuned to get the emitted signal in the 1982 nm window suitable for water vapor and HDO isotopic ratio sounding. The idler wave is generated in the 2290 nm window suitable for CH_4 probing. The second NesCOPO QPM condition is tuned for signal emission in the CO_2 2051 nm window (R30 absorption line). A specific pumping timing is applied to operate in double-pulse mode (i.e. 75 Hz double-pulse emission) with a 500 µs delay. This way, each OPO can be switched from the OFF to the ON line within 500 µs, which is much shorter than the coherence time of the atmosphere, even under a strong wind or a strong turbulence. The idler beams are coupled out and combined with dichroic mirrors to be sent to the OPA line.

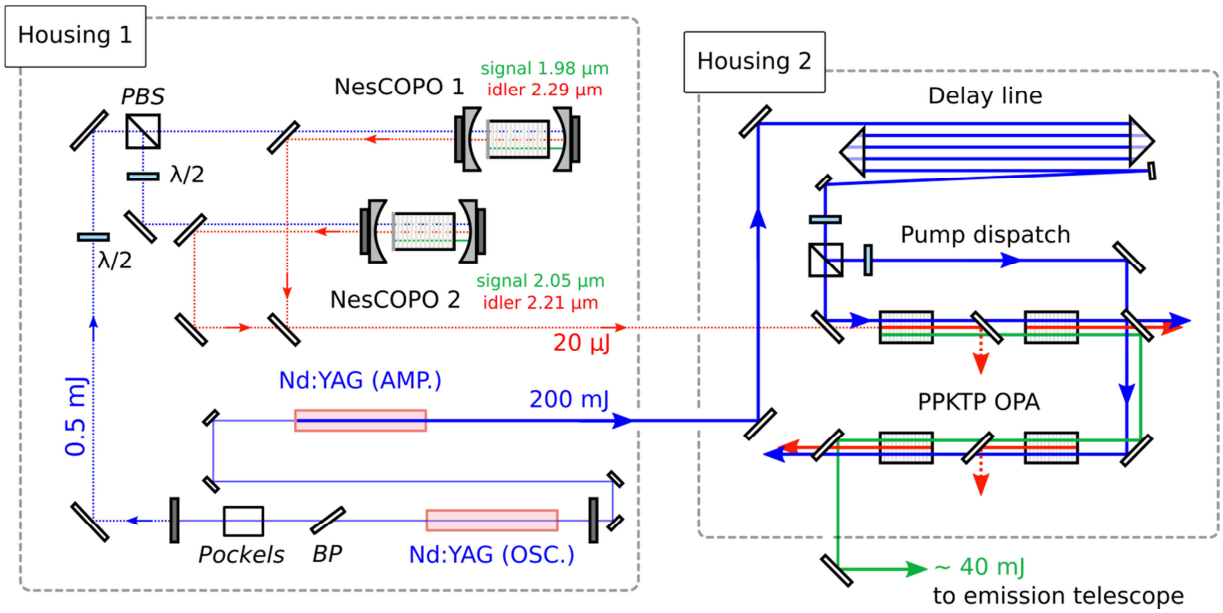

Figure 8. Simplified optical layout of the 2 µm emitter for airborne operation. (PBS) stands for polarizing beam splitter, (λ/2) for half-wave plate, and (BP) for Brewster plate.

The OPA line is composed of cascaded Rb:PPKTP nonlinear crystals with transverse aperture of 5 x 5 mm². The OPA has been designed to amplify the extracted idler energy from the NesCOPO from ~20 µJ to several tens of mJ (gain > 30 dB). We chose to keep the same beam diameter size of 2.9 mm diameter in all crystals, to reduce the footprint of the pump distribution stages, and limited the fluence to 2.5 J/cm² to eliminate the risk of laser-induced damage. To switch from CO_2 to H_2O, the PPRKTP crystal temperature has to be changed by 25 °C. The idler wave is removed after each crystal as it is an efficient way to reduce saturation and back-conversion effects, optimizing the extracted signal energy and M^2. The OPA is pumped by the 1.064 µm beam after amplification in a Nd:YAG rod to reach 200 mJ energy per pulse.

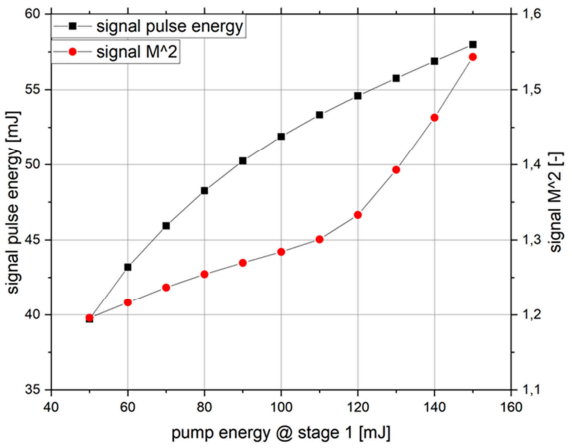

(a)

(b)

Figure 9. (a) Signal beam energy and M² calculated at the output of the OPA line as a function of pump energy in the first OPA stage. The configuration is composed of two stages with two PPKTP crystals in each stage and idler filtering. The total pump energy distributed in the OPA line (stage 1+2) is 200 mJ. (b). Picture of 4 PPKTP crystals.

Special care has been taken with the thermo-mechanical management of the laser and OPOs in order to withstand temperature changes and the expected aircraft environment (ATR 42 aircraft from the SAFIRE fleet). The housing is made from a single block of aluminum with thicknesses validated by the laser manufacturer. The NesCOPO cavity is inside an opto-mechanic assembly built around a low expansion glass frame with stringent mechanical alignment tolerances. The NesCOPOs are located in the same housing as close as possible to the laser oscillator in order to minimize pump beam pointing fluctuations. The housing is mounted on a specially damped carbon breadboard via isostatic mounts. The design has been validated by FEM simulation of thermal deformations and vibrational modes, and a CAD view can be seen in Figure 10.

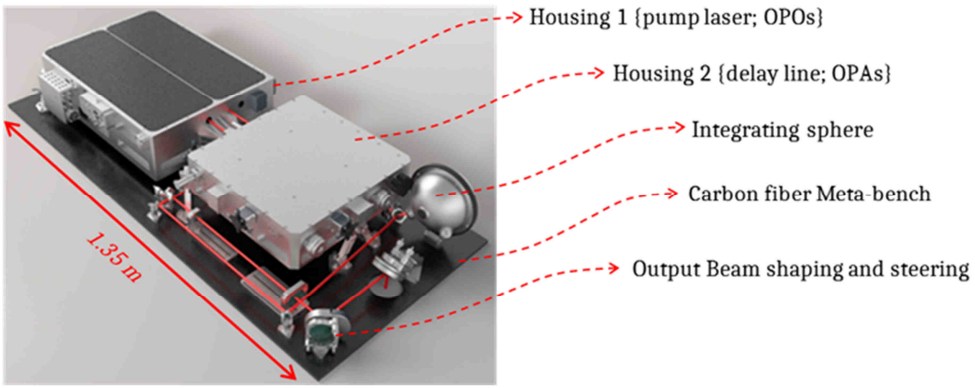

Figure 10. Overall emitter layout on carbon breadboard, together with emission beam shaping and energy calibration systems.

The same care has been taken with the receiver of the lidar. The telescope, that includes a 35 cm diameter mirror, has been manufactured by a specialized company, and will be integrated in a carbon and steel frame mounted on dampers, designed to withstand the vibrations of the plane.

For this lidar, we chose an innovative wavelength measurement solution, which should provide a much better precision than the traditional one based on Fizeau interferometers. It consists in using a GPS-disciplined and CEO-stabilized frequency comb and beat note analysis in order to retrieve the optical frequency. To perform this optical beating, a leak from the OPA stages is extracted and sent into a second harmonic generation (SHG) stage in order to match the spectral range of the frequency comb.

More details on this lidar have been given in a recent publication [18].

3.3. LWIR emitter with a tunable pump laser

The leading idea of this emitter design was to downconvert to the LWIR directly from 2 µm laser radiation, using the "LWIR MOPA" design of Figure 5. Indeed, the optical efficiency of this solution is, in principle, twice the one of the "2 µm MOPA+DFG" design. This development has only been possible thanks to the commercial availability of 2 µm optical components and systems such as thulium and holmium doped lasers, 2 µm optics, 2 µm single mode fibers and fibered components, InGaAs detectors, InGaAs spectrometers, etc.

First, two single-longitudinal-mode lasers were developed specifically for OPO pumping, using thulium doped yttrium aluminium perovskite (Tm^{3+}:YAP) as the laser medium. The first version was passively Q-switched, and emitted 36 ns long pulses with an energy of 170 µJ at 1940 nm [19]. Later, a 125 µm étalon was added to make the laser run on a single longitudinal mode (unpublished). Later, an actively Q-switched, wavelength-tunable laser was developed [20]. It emits 60 to 80 ns long pulses with an energy of 250 µJ at a 1 kHz repetition rate, with a TEM_{00} mode and a M^2 factor below 1.05. The laser runs on a single longitudinal mode thanks to the combination of a volume Bragg grating (VBG) and a 4-mm uncoated YAG étalon. The output wavelength is tunable from 1940 nm to 1960 nm by translating the VBG owing to a transverse chirp of the Bragg period in the VBG. However, since the étalon is not moved synchronously, the laser tunes by hops of one cavity free spectral range (0.65 cm^{-1}).

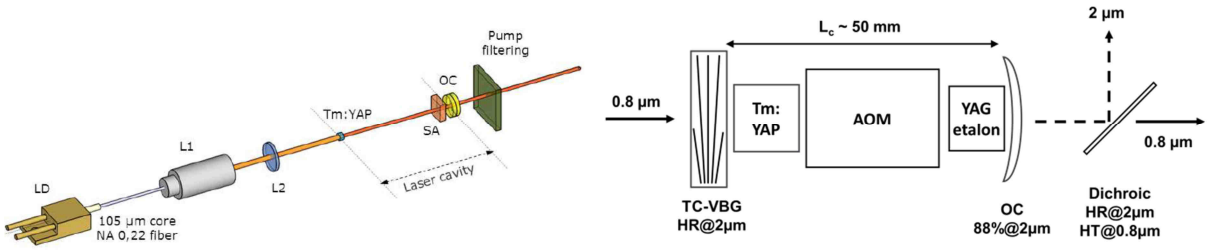

Figure 11. Q-switched Tm:YAP lasers developed by partners (Thales R&T and SME *teem photonics*) for OPO pumping. Left: passively Q-switched. Right: actively Q-switched Tm:YAP laser with a transversally-chirped VBG enabled wavelength tunability.

Secondly, we developed a LWIR version of the NesCOPO, by using OP-GaAs [21] as the nonlinear medium. The difficulty to manufacture the crystals did not leave time for coating the M_2 mirror directly on the crystal facet, so we used an external mirror instead (Figure 12). For the same reasons we did not polish a wedged output facet to control the nonlinear phase (see Sec. 5). Nonetheless the NesCOPO could be arbitrarily tuned to any desired wavelength by combining piezoelectric actuation and temperature control, the spectral purity was almost Fourier-transform-limited, and a spectrum of ammonia near 10.4 µm was recorded [22]. One of the positive outcomes of these experiments involving the first version of the Tm:YAP laser was the very good reproducibility of the results over the years, secured by the long lifetime of components in the infrared and the good opto-mechanical implementation made by the partner company.

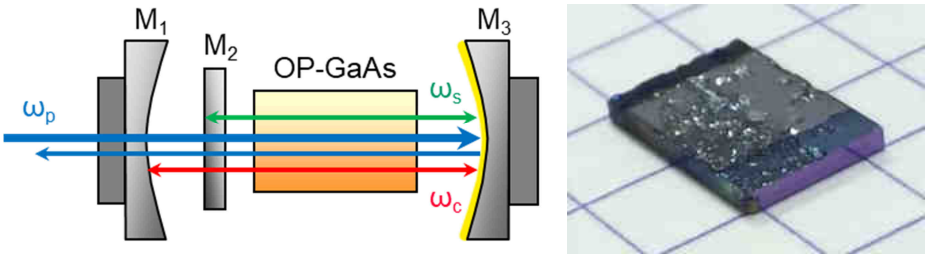

Figure 12. Schematic of the NesCOPO cavity used for LWIR generation. Right: picture of an OP-GaAs crystal with two different QPM periods.

The complete optical setup of the LWIR emitter is shown in Figure 13a. Approximately 25 µJ are used to pump the OPO, 90 µJ for the SFG/SHG stage (described later), and the rest goes into the OPA. In the second version of the pump

laser, a parametric amplifier (OPA), active Q-switching and wavelength tunability have been added. Active Q-switching was requested to increase the pulse energy to 250 µJ to have at least 120 µJ left to pump the OPA, increase the average power to reduce the integration time of the wavelength meter, and increase the repetition rate for lidar measurements. Also, active Q-switching allows synchronization with other lasers, for simultaneous wavelength emission or further amplification of the LWIR with another pump laser. Tunability of the pump wavelength (provided by a VBG mounted on a linear piezoelectric stage) has been added to tune the idler wavelength on a broad range faster than temperature control.

Figure 13b shows the idler wavelength tunability triggered by the pump laser tunability. The idler/pump tunability slope ω_i/ω_p is very close to 1. It is thus expected that the NesCOPO will tune by mode hops over the same amount as the pump in average, i.e. 0.65 cm^{-1}, with an added, unpredictable deviation allowed by Vernier mode selection within the parametric gain bandwidth, which is about 14 cm^{-1} wide for a 6-mm-long OP-GaAs crystal with a double-pump pass. More precise characterizations are in progress. Of course, the more traditional tuning methods described in Sec. 2.2 are still operative.

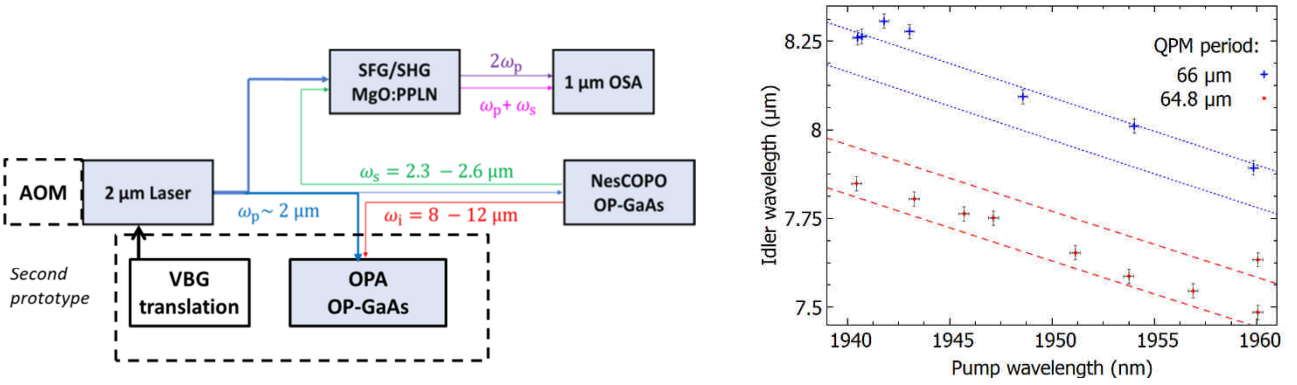

(a) (b)

Figure 13. (a) schematic of the LWIR emitter. The dashed rectangles are functions added in the most recent version of the emitter. (b) Idler wavelength versus pump wavelength when translating the TC-VBG inside the pump laser, for two QPM periods. The dashed lines indicate the theoretical extremes of the parametric gain bandwidth.

To measure the idler wavelength, we could have used a commercial wavemeter based on Fizeau interferometers, as they are also available in the LWIR. Instead, we chose a more compact and less expensive solution based on sum frequency generation (SFG) of the pump and signal wavelengths towards 1 µm where a silicon based spectrometer can be used. The pump frequency can also be measured by second harmonic generation (SHG). The idler wavelength is then retrieved from the equation: $\omega_\mathrm{i} = \omega_\mathrm{SHG} - \omega_\mathrm{SFG}$. Over short time periods, the wavelength of the pump is much more stable than that of the idler, which is likely to be tuned, switched, or servo-locked by the user. So only the SFG needs to be constantly recorded, so that the idler wavelength is deduced from: $\omega_\mathrm{i} = 2\omega_\mathrm{p} - \omega_\mathrm{SFG}$.

Sum frequency generation was obtained in a 20-mm-long MgO:PPLN crystal with an apodized, longitudinally chirped poling (APPLN). The purpose of the chirp is to increase the acceptance bandwidth to avoid having to move or heat the crystal when the idler wavelength is tuned. The crystal was manufactured with 6 different aperiodic QPM tracks with different center period and chirp rates, to minimize the risks related to the exact prediction of the conversion efficiency, which scales down with the acceptance bandwidth. The chosen chirp was 0.25 µm/mm, yielding a SFG bandwidth of 150 cm^{-1} around 2.5 µm. SHG of the pump is then the consequence of off-phase-matched conversion in the crystal enabled by a high pump fluence. Achieving the same in a PPLN would have required a length of no more than 2 mm, resulting in a very low efficiency. In a birefringence phase matched crystal, finding a giant acceptance would have been a stroke of luck and in any case the small beam sizes would have been incompatible with walk-off. This is a good example of the many possibilities offered by QPM that we introduced in Sec. 2.1.

More details on this emitter will be presented and published elsewhere [23].

We recently integrated the first version of the LWIR emitter in a complete lidar system mounted on a wheeled camera dolly. We used the lidar to detect chemical warfare agents on French military ground. The system proved to be very robust, and we now aim at duplicating the LWIR source to emit ON/OFF pulses in a row.

4. CONCLUSION

Standoff gas sensing with lidars is a very demanding niche for laser technologies, with sometimes conflicting requirements. The wavelength must be very stable *and* be tuned over a large range ; the radiation should be pulsed and the linewidth be very narrow *and* stable over the pulses ; the pulses should be emitted closely in time *while* there is very few metrology tools for pulsed radiation ; the laser should emit several watts *and* fit in a shoebox.

In an attempt to meet these needs, we have developed parametric down-conversion sources that are versatile enough to meet the requirements of many different applications: ground-based and airborne greenhouse gases monitoring (aiming to get spaceborne one day), methane leak detection, and chemical warfare agents detection. They rely on state-of-the-art technologies such as quasi-phase matched materials, single-frequency lasers, frequency-agile lasers, infrared spectrometers, and on the partners developing them.

We are constantly looking for new solutions to simplify the optical setup without compromising the performance. InGaAs and HgCdTe avalanche photodiodes, new quasi-phase matching schemes, upconversion detectors, tunable fibered lasers, compact frequency comb lasers, infrared semiconductor lasers, are some examples of possible game changers for gas detection lidars. The good health of the photonic industry is also a stepping stone of our developments.

ACKNOWLEDGEMENTS

The authors would like to thank Julien Totems and Patrick Chazette (LSCE, France), Cyrille Flamant (LATMOS, France), Nicolas Blouzon and Nicolas Geyskens (DT INSU, France), Corinne Evesque (IPSL, France) Bruno Grouiez and Laurence Régalia (GSMA, France), for their contribution to WaVIL, the H_2O/HDO lidar.

They are also grateful to Jan Fabian Geus and Michael Strotkamp (Fraunhofer ILT, Germany), Andrius Zukauskas, Kjell Martin Mølster, Carlota Canalias and Valdas Pasiskevicius (KTH, Sweden), Lukas Nagy, Oliver Pitz, David Fehrenbacher, Hanjo Schaefer, and Dirk Heinecke (Spacetech GmbH, Germany), Paul Denk and Norbert Graf (Innolas, Germany), Marine Dalin and Vincent Lebat (Onera, France), for their contribution to LEMON, the airborne multispecies lidar.

The authors show appreciation to Basile Faure, Grégoire Shouaité, and Marine Favier from teem photonics, Arnaud Grisard and Eric Lallier at Thales R&T, and Bruno Gérard at Thales III-V lab, for their long-lasting cooperation in building MUSTARD and SPICE, the LWIR emitters.

This work has been funded by French Agence Nationale pour la Recherche ANR under grant N° ANR-16-CE01-0009 (WaVIL), European Union’s Horizon 2020 research and innovation program under grant agreement N° 821868 (LEMON), Direction Generale de l'Armement (DGA) and ANR under grant ANR-11-ASTR-016 (MUSTARD), DGA under contract 172906033 (SPICE).

REFERENCES

[1] B. J. Orr, "Infrared LIDAR Applications in Atmospheric Monitoring," in *Encyclopedia of Analytical Chemistry*, R. Meyers, Ed., 2017.

[2] G. Ehret, C. Kiemle, M. Wirth, A. Amediek, A. Fix and S. Houweling, "Space-borne remote sensing of CO2, CH4, and N2O by integrated path differential absorption lidar: a sensitivity analysis," *Applied Physics B: Lasers and Optics*, vol. 90, no. 3, p. 593–608, 2008.

[3] V. Pasiskevicius and C. Canalias, "Mirrorless optical parametric oscillator," *Nature Photonics*, vol. 1, p. 459–462, 2007.

[4] A. Godard, M. Raybaut and M. Lefebvre, "Nested Cavity Optical Parametric Oscillators – A Tunable Frequency Synthesizer for Gas Sensing," in *Encyclopedia of Analytical Chemistry*, John Wiley & Sons, Ltd, 2017.

[5] "HighFinesse lambdameters," 2021. [Online]. Available: https://www.highfinesse.com/en/wavelengthmeter/.

[6] J. G. des Aulnois, B. Szymanski, A. Grimieau and L. Sillard, "A new way of controlling NesCOPOs (nested cavity doubly resonant OPO) for faster and more efficient high resolution spectrum measurement," in *Nonlinear Frequency Generation and Conversion: Materials and Devices XVII*, 2018.

[7] E. le Coarer, J. Ferrand, J. Boussey, S. Blaize, L. G. Venancio, P. Kern, P. Puget, M. Ayraud, C. Bonneville, B. Demonte, A. Morand, D. Barbier and T. Gonthiez, "SWIFTS: on-chip very high spectral resolution spectrometer," in *International Conference on Space Optics (ICSO 2010)*, 2017.

[8] J. B. Dherbecourt, M. Raybaut, J. M. Melkonian, J. Hamperl, R. Santagata, M. Dalin, V. Lebat, A. Godard, C. Flamant, J. Totems, P. Chazette, V. Pasiskevicius, D. Heinecke, H. Schäfer, M. Strotkamp, J. F. Geus, S. Rapp, H. Sodemann and H. C. Steen-Larsen, "Design and pre-development of an airborne multi-species differential absorption lidar system for water vapor and HDO isotope, carbon dioxide, and methane observation," in *International Conference on Space Optics (ICSO 2020)*, 2021.

[9] A. Kabacinski, J. Armougom, J.-M. Melkonian, M. Raybaut, J.-B. Dherbecourt, A. Godard, R. Vasilyeu and V. Smirnov, "Wavelength tunable, single-longitudinal-mode optical parametric oscillator with a transversally chirped volume Bragg grating," January 2020.

[10] M. W. Haakestad, G. Arisholm, E. Lippert, S. Nicolas, G. Rustad and K. Stenersen, "High-pulse-energy mid-infrared laser source based on optical parametric amplification in ZnGeP2," *Optics Express*, vol. 16, p. 14263–14273, 2008.

[11] J.-M. Melkonian, J. Armougom, M. Raybaut, J.-B. Dherbecourt, G. Gorju, N. Cézard, A. Godard, V. Pašiškevičius, R. Coetzee and J. Kadlčák, "Long-wave infrared multi-wavelength optical source for standoff detection of chemical warfare agents," *Appl. Opt.*, vol. 59, p. 11156–11166, December 2020.

[12] H. C. Steen-Larsen, C. Risi, M. Werner, K. Yoshimura and V. Masson-Delmotte, "Evaluating the skills of isotope-enabled general circulation," *J. Geophys. Res. Atmospheres*, vol. 122, p. 246–263, 2017.

[13] J. Hamperl, C. Capitaine, J.-B. Dherbecourt, M. Raybaut, P. Chazette, J. Totems, B. Grouiez, L. Régalia, R. Santagata, C. Evesque, J.-M. Melkonian, A. Godard, A. Seidl, H. Sodemann and C. Flamant, "Differential absorption lidar for water vapor isotopologues in the 1.98 µm spectral region: sensitivity analysis with respect to regional atmospheric variability," vol. 14, pp. 6675-6693.

[14] M. Raybaut, T. Schmid, A. Godard, A. K. Mohamed, M. Lefebvre, F. Marnas, P. Flamant, A. Bohman, P. Geiser and P. Kaspersen, "High-energy single-longitudinal mode nearly diffraction-limited optical parametric source with 3 MHz frequency stability for CO2 DIAL," *Optics Letters*, vol. 34, p. 2069–2071, 2009.

[15] J. Dherbecourt, J. Melkonian, A. Godard, V. Lebat, N. Tanquy, C. Blanchard, X. Watremez, D. Dubucq, S. Doz, P. Foucher and M. Raybaut, "The NAOMI GAZL multispecies differential absorption lidar: realization and testing on the TADI gas leak simulation facility," in *Conference on Lasers and Electro-Optics (CLEO)*, 2019.

[16] A. Zukauskas, N. Thilmann, V. Pasiskevicius, F. Laurell and C. Canalias, "5 mm thick periodically poled Rb-doped KTP for high energy optical parametric frequency conversion," *Optical Materials Express*, vol. 1, p. 201–206, June 2011.

[17] [Online]. Available: https://lemon-dial-project.eu/.

[18] J. Hamperl, J. Geus, K. Mølster, A. Zukauskas, J.-B. Dherbecourt, V. Pasiskevicius, L. Nagy, O. Pitz, D. Fehrenbacher, H. Schaefer, D. Heinecke, M. Strotkamp, S. Rapp, P. Denk, N. Graf, M. Dalin, V. Lebat, R. Santagata, J.-M. Melkonian, A. Godard, M. Raybaut and C. Flamant, "High Energy Parametric Laser Source and Frequency-Comb-Based Wavelength Reference for CO2 and Water Vapor in the 2 µm Region: Design and Pre-Development Experimentations," *Atmosphere*, vol. 12, p. 402, 2021.

[19] A. Grisard, B. Faure, G. Souhaité and E. Lallier, "High energy single frequency passively Q-switched 2-micron microlaser in thulium-doped yttrium aluminium perovskite," in *Advanced Solid State Lasers*, 2014.

[20] Q. Berthomé, A. Grisard, B. Faure, G. Souhaité, E. Lallier, J.-M. Melkonian and A. Godard, "Actively Q-switched tunable single-longitudinal-mode 2 µm Tm:YAP laser using a transversally chirped volume Bragg grating," *Opt. Express*, vol. 28, p. 5013–5021, February 2020.

[21] A. Grisard, E. Lallier and B. Gérard, "Quasi-phase-matched gallium arsenide for versatile mid-infrared frequency

conversion," *Optical Materials Express*, vol. 2, p. 1020, July 2012.

[22] J. Armougom, J.-M. Melkonian, J.-B. Dherbecourt, M. Raybaut, A. Grisard, E. Lallier, B. Gérard, B. Faure, G. Souhaité, B. Boulanger and A. Godard, "A narrowband infrared source based on orientation-patterned GaAs for standoff detection of chemicals," *Applied Physics B*, vol. 124, p. 133, 14 June 2018.

[23] Q. Berthomé, B. Faure, G. Souhaité, M. Jean-Michel, M. Raybaut, A. Godard, A. Grisard and É. Lallier, "Widely tunable LWIR parametric source," in *10th International Symposium on Optronics in defence & security (OPTRO)*, Paris, 2022.